Published in final edited form as:
Science. 2013 November 1; 342(6158): . doi:10.1126/science.1241974.

On and Off Retinal Circuit Assembly by Divergent Molecular Mechanisms

Lu O. Sun[1,2], **Zheng Jiang**[1,*], **Michal Rivlin-Etzion**[3,*,†], **Randal Hand**[1,2], **Colleen M. Brady**[1,2], **Ryota L. Matsuoka**[1,2,‡], **King-Wai Yau**[1], **Marla B. Feller**[3], and **Alex L. Kolodkin**[1,2,§]

[1]Solomon H. Snyder Department of Neuroscience, The Johns Hopkins University School of Medicine, Baltimore, MD 21205, USA

[2]Howard Hughes Medical Institute, Baltimore, MD 21205, USA

[3]Department of Molecular and Cell Biology and the Helen Wills Neuroscience Institute, University of California, Berkeley, Berkeley, CA 94720, USA

Abstract

Direction-selective responses to motion can be to the onset (On) or cessation (Off) of illumination. Here, we show that the transmembrane protein semaphorin 6A and its receptor plexin A2 are critical for achieving radially symmetric arborization of On starburst amacrine cell (SAC) dendrites and normal SAC stratification in the mouse retina. Plexin A2 is expressed in both On and Off SACs; however, semaphorin 6A is expressed in On SACs. Specific On-Off bistratified direction-selective ganglion cells in *semaphorin 6A*$^{-/-}$ mutants exhibit decreased tuning of On directional motion responses. These results correlate the elaboration of symmetric SAC dendritic morphology and asymmetric responses to motion, shedding light on the development of visual pathways that use the same cell types for divergent outputs.

The detection of object motion is a critical visual function. Direction-selective responses to visual cues by the vertebrate retina depend on the precise wiring of inhibitory starburst amacrine cells (SACs) onto direction-selective ganglion cells (DSGCs) (1–4). SACs are divided into onset (On) and cessation (Off) subtypes based on their function, which correlates with localization of their cell bodies and dendritic processes (5). On and Off SACs costratify with distinct DSGC dendritic arborizations that have the capacity to mediate On or Off directional responses (6–8), and SACs play a fundamental role in regulating DSGC output (9–12). Protocadherins mediate the self-avoidance of SAC dendrite processes and regulate the morphogenesis of both On and Off SACs (13). However, the molecular mechanisms that specify On versus Off SACs, and the signaling pathways governing the functional assembly of retinal direction-selective circuitry, remain unclear.

[§]Corresponding author. kolodkin@jhmi.edu.
[*]These authors contributed equally to this work
[†]Present address: Department of Neurobiology, Weizmann Institute of Science, Rehovot 76100, Israel.
[‡]Present address: Department of Developmental Genetics, Max Planck Institute for Heart and Lung Research, 61231 Bad Nauheim, Germany.

Supplementary Materials
www.sciencemag.org/content/342/6158/1241974/suppl/DC1
Materials and Methods
Figs. S1 to S17
Movies S1 to S6
References (26–35)

Class A plexin receptors (PlexAs) in the developing mouse retina are expressed largely in the inner plexiform layer (14, 15). To identify cell types expressing PlexA2, we performed double immunohistochemistry analyses and observed co-localization of PlexA2 and choline acetyltransferase (ChAT), which is expressed by SACs (Fig. 1, A to C). This observation was confirmed by in situ hybridization analysis (fig. S1, A and C) and by labeling in a *PlexA2-LacZ* reporter mouse (fig. S2, F to I). The protein distributions in the inner plexiform layer of PlexA2 and semaphorin 6A (Sema6A), a transmembrane semaphorin that is a functional PlexA2 ligand in the mammalian nervous system (16, 17), are complementary with respect to PlexA2 expression in the Off region of the inner plexiform layer, but they exhibit selective overlap in the On region of the inner plexiform layer (Fig. 1, D to F, and fig. S1, E to H″). Sema6A immunoreactivity accumulates along the inner of the two PlexA2-immunopositive (PlexA2$^+$) sublaminae, is observed in On but not Off inner plexiform layer neurites, and is found in the cell bodies of all PlexA2$^+$ cells in the ganglion cell layer but not the inner nuclear layer (Fig. 1, G to I). Thus, Sema6A and PlexA2 are coexpressed in On, but not Off, SACs.

To investigate the functional importance of this selective PlexA2 and Sema6A protein localization, we isolated SACs from a mouse line, *ChAT::cre;ROSA*$^{LSL\text{-}Tdtomato}$, in which both On and Off SACs are genetically labeled with Tdtomato (fig. S3, A to C), and cultured them in vitro on stripes coated with recombinant Sema6A-Fc protein. As we observed in vivo, there are two populations of SACs in culture: Sema6A-positive (Sema6A$^+$) and Sema6A$^-$ SACs (fig. S1, I to K″). Neurites from wild-type Sema6A$^-$ SACs avoid Sema6A-Fc stripes, whereas wild-type Sema6A$^+$ SACs show no preference and extend their processes freely over Sema6A-Fc and control stripes (Fig. 1, J to K′ and N). In contrast, both Sema6A$^-$ and Sema6A$^+$ SACs derived from *PlexA2*$^{-/-}$ mutant retinas extend neurites equally over Sema6A-Fc and control stripes (Fig. 1, L to N), showing that in vitro exogenous Sema6A repels processes only from SACs that express PlexA2 but not Sema6A —the expression profile of Off SACs in vivo.

To address PlexA2 function in retinal development in vivo, we first characterized SAC sublaminar neurite stratification and SAC cell body mosaic patterning in *PlexA2*$^{-/-}$ retinas. SACs normally stratify in two discrete inner plexiform layer laminae: S2 and S4 (Fig. 2A). In *PlexA2*$^{-/-}$ retinas, however, these two stratifications fail, with full penetrance, to completely segregate from each other (Fig. 2B, and fig. S4, A and A′; $n = 6$ *PlexA2*$^{-/-}$ mutants). This is in contrast to calretinin$^+$ amacrine cells and retinal ganglion cells, TH$^+$ and vGlut3$^+$ amacrine cells, and NK3R$^+$, Syt2$^+$, and PKCα$^+$ bipolar cells, all of which show normal axonal targeting and dendritic stratifications in the *PlexA2*$^{-/-}$ retina (fig. S4, B to G′). In addition, *PlexA2*$^{-/-}$ On and Off SACs exhibit indistinguishable density recovery profiles, and several additional cell body mosaic spacing parameters, compared with control SACs (fig. S5), showing that PlexA2 is dispensable for regulating SAC cell body mosaic spacing.

The in vivo protein distribution of PlexA2 and Sema6A in the inner plexiform layer, and the responses to Sema6A protein by SAC neurites in vitro (Fig. 1), suggest that Sema6A is involved in PlexA2-dependent SAC dendritic stratification. We tested this idea by analyzing *Sema6A*$^{-/-}$ mutant retinas and found that *PlexA2*$^{-/-}$ SAC dendritic stratification defect is phenocopied, with full penetrance and expressivity, in *Sema6A*$^{-/-}$ retinas (Fig. 2C; $n = 6$ *Sema6A*$^{-/-}$ mutants) and is not further enhanced in *PlexA2*$^{-/-}$;*Sema6A*$^{-/-}$ double mutant retinas (*dKO*) (Fig. 2, D and H; $n = 4$ *PlexA2*$^{-/-}$;*Sema6A*$^{-/-}$ mutants). This suggests that *PlexA2* and *Sema6A* are involved in the same signaling pathway that regulates SAC dendritic stratification in the inner plexiform layer (Fig. 2G). To determine whether the segregation of On and Off SAC processes is cell-type–autonomous, we generated a *ChAT::cre;PlexA2*$^{F/-}$ mouse line in which PlexA2 is selectively ablated in all SACs (fig. S2,

J to M). We observed in these mutant retinas the same stratification defects we found in *PlexA2*$^{-/-}$ mice (Fig. 2, E, F, and H, and fig. S2, J′ to M′). SAC dendritic stratification defects were not observed in other *PlexA* null mutant mice (*PlexA1*$^{-/-}$, *PlexA3*$^{-/-}$, and *PlexA4*$^{-/-}$) (fig. S6, A to C) or *neuropilin-1* and *-2* deficient mice (fig. S6, D to F), suggesting that most secreted semaphorins do not mediate SAC stratification. The same is true for mutants in the genes encoding the remaining class 6 semaphorin proteins (*Sema6B, 6C,* and *6D*) (18).

In early postnatal development, wild-type On and Off SAC processes are initially entangled at P0 and P2 but segregate into two distinct stratifications by P4 (Fig. 2I to K′) (6, 19). We found that On and Off SAC dendrites in *ChAT::cre;ROSA*$^{LSL\text{-}Tdtomato}$ *PlexA2*$^{-/-}$ mice failed to completely segregate by P4 (Fig. 2, O and O′). To further investigate these SAC dendritic process stratification defects, in which On and Off SAC processes apparently cross over between inner plexiform layers 2 and 4, we analyzed sparsely labeled SACs in *ChAT::cre*^{ER}*;ROSA*$^{LSL\text{-}Tdtomato}$*; PlexA2*$^{-/-}$ mutant retinas. We observed that dendrites of both On and Off SACs stratify normally in control retinas (*PlexA2*$^{+/-}$) but that both SAC types can stratify inappropriately in the *PlexA2*$^{-/-}$ mutants (fig. S3). We examined 35 *PlexA2*$^{-/-}$ SAC processes that crossed between the On and Off ChAT bands and traced 17 of these to Off SACs and 18 to On SACs (fig. S3, D to L). Therefore, both in vitro and in vivo observations support the idea that Sema6A-PlexA2 repulsive interactions are a critical component of the molecular mechanisms that underlie stratification of On and Off SAC dendritic processes.

The formation of distinct On and Off SAC sublaminar dendritic process stratifications during early retinal development differentiates these two motion-detection circuits. Because Sema6A is expressed selectively and continuously in On, but not Off, SACs (Fig. 1 and fig. S1), we next asked if Sema6A-PlexA2 signaling functions later in retinal development to refine direction-selective circuitry by regulating On SAC dendritic morphology. To visualize On SAC dendritic morphology, we filled individual adult On SACs with Alexa-555 dye and confirmed their identity by anti-ChAT immunostaining (fig. S7, A to C). Wild-type On SACs exhibited characteristic radially symmetric morphology (Fig. 3A), whereas *PlexA2*$^{-/-}$ On SACs were missing extensive portions of their dendritic fields (Fig. 3B). Also, normal SAC dendritic self-avoidance was compromised in *PlexA2*$^{-/-}$ On SACs (Fig. 3, A′ and B′, and fig. S7, D to G). Unlike SAC self-avoidance defects previously described in protocadherin mutants (13), the *PlexA2*$^{-/-}$ defects were confined to the distal-most third of SAC dendritic processes. These same defects were found in *Sema6A*$^{-/-}$ and *PlexA2*$^{-/-}$;*Sema6A*$^{-/-}$ mutants (Fig. 3, C toD′). Quantification of total dendritic length (Fig. 3E), dendritic field area (Fig. 3F), self-crossing number per SAC (Fig. 3G), symmetry index (Fig. 3H; defined in fig. S7I), and dendritic complexity (Sholl analysis, Fig. 3I) reveals that the overall dendritic arborization characteristics and symmetric dendritic organization are compromised in *PlexA2*$^{-/-}$, *Sema6A*$^{-/-}$, and *PlexA2*$^{-/-}$;*Sema6A*$^{-/-}$ mutants.

In the developing rabbit retina, On SAC dendritic processes achieve symmetry by postnatal day 0 (P0) (20). In addition to our Alexa-555 injection experiments in adult mice, we used genetic sparse labeling to delineate On SAC morphology throughout postnatal murine retinal development. Wild-type On SACs exhibit asymmetric dendritic morphology at P0 and P2 (Fig. 3J and fig. S8A, top left panels) and display extensive dendritic process motility early postnatally (movie S1). As early as P4, however, symmetric radial dendritic process organization was achieved (Fig. 3K and fig. S8A, bottom left panels) and then maintained throughout retinal development (Fig. 3, L to N). At P0, *PlexA2*$^{-/-}$ On SAC dendrites resemble wild-type with respect to dendritic asymmetry and other dendritic organization parameters (Fig. 3, J′ and N, $P = 0.9884$; and fig. S8, A and B); they also exhibit similar dendritic process motility (movie S2). Nonetheless, they still retain asymmetric dendritic

morphology at P4 (Fig. 3, K′ and N, $P < 0.001$; and fig S8A, bottom right panels) or even later (P14 and P21) (Fig. 3, L′, M′, and N, $P < 0.001$; and fig. S8C). These same defects apply to *Sema6A*$^{-/-}$ mutant retinas (fig. S9). We did not observe any correlation between SAC dendritic asymmetry phenotypes and the overall location of On SAC cell bodies in *PlexA2*$^{-/-}$ retinas; *PlexA2*$^{-/-}$ On SACs in all four retinal quadrants exhibit the full range of dendritic process symmetry defects (fig. S10). Thus, in addition to contributing to the separation between On and Off SAC dendritic stratifications into distinct inner plexiform layer laminae, Sema6A-PlexA2 signaling regulates the elaboration of symmetric On SAC dendritic fields during postnatal retina development.

To investigate whether *PlexA2*$^{-/-}$ On SAC inner plexiform layer dendritic arborization phenotypes in the *x-y* plane (Fig. 3) are correlated with SAC dendritic stratification defects in the *z* plane of the inner plexiform layer (Fig. 2, A to D), we analyzed both the *x-y* projection images and *z*-stacked images of individual, genetically labeled, *PlexA2*$^{-/-}$ On SACs. We found two classes of *PlexA2*$^{-/-}$ On SACs: (i) those that stratify normally within the ChAT^{+} On sublaminae (11 out of 29 On SACs) (fig. S11, B and B′), and (ii) those that misstratify within the ChAT^{+} Off sublaminae (18 out of 29 On SACs) (fig. S11, C and C′). However, whether these *PlexA2*$^{-/-}$ mutant SACs exhibit normal or aberrant dendritic stratification within the ChAT^{+} sublaminae, they show the same dendritic field symmetry defects (fig. S11, Dto G, and movie S3). Thus, *PlexA2*$^{-/-}$ On SAC dendritic arborization phenotypes in the *x-y* plane are distinct from SAC dendritic stratification defects in the *z* plane.

The restricted expression of Sema6A in On SACs raises the possibility that Sema6A regulates only On, but not Off, SAC dendritic arborization in the *x-y* plane. In contrast, protocadherins expressed in both On and Off SACs (21) dictate dendritic self-avoidance in both cell types (13). We investigated this issue by examining genetically labeled Off SACs. Indeed, *Sema6A*$^{-/-}$ Off SACs (Fig. 4D) exhibit the normal, radially symmetric, dendritic morphology found in wild-type SACs (Fig. 4, A and A′, quantified in Fig. 4H, and movie S4). *Sema6A*$^{-/-}$ Off SACs also have normal dendritic field area, but *Sema6A*$^{-/-}$ On SACs are abnormal (Fig. 4, D′ and G). *PlexA2*$^{-/-}$ Off SACs (figs. S12 and S13 and Fig. 4H) exhibit symmetric dendritic fields, both within and outside of regions where On and Off SAC dendrites fail to separate from one another (fig. S11H). Reconstruction of individual *PlexA2*$^{+/-}$ and *PlexA2*$^{-/-}$ Off SAC dendritic arbors further illustrates that a fraction of mutant Off SAC dendritic processes from an individual SAC can stratify within the ChAT^{+} On sublamina without affecting the symmetric morphology of the entire Off SAC dendritic arbor (movies S5 and S6). We observed that *PlexA2*$^{-/-}$ On SACs show a modest reduction in dendritic field area (Fig. 4G and fig. S13H), suggesting that PlexA2 may promote dendritic-process outgrowth in Off SACs.

The dendritic arborization defects observed in individual *Sema6A*$^{-/-}$ and *PlexA2*$^{-/-}$ mutant SACs can be generalized to the overall On SAC dendritic plexus organization. Using anti-ChAT immunostaining to label all On and Off SAC dendritic processes, we observed that only On SAC dendritic plexuses are defective in *Sema6A*$^{-/-}$ retinas (compare Fig. 4E′ with Fig. 4, B, B′, and E; quantification in fig. S12G). Large gaps and holes in the ChAT^{+} plexuses were found in areas where *Sema6A*$^{-/-}$ On SACs failed to elaborate their dendrites (compare Fig. 4F′ with Fig. 4, C, C′, and F). The organization of the On SAC dendritic plexus is not likely mediated by the other Sema6 proteins because *Sema6B*$^{-/-}$ and *Sema6C*$^{-/-}$;*Sema6D*$^{-/-}$ double mutants exhibit normal On and Off SAC plexus organization (fig. S14C; quantification in fig. S14D). Defects in the *PlexA2*$^{-/-}$ ChAT^{+} On plexus phenocopy those observed in *Sema6A*$^{-/-}$ mutants (fig. S12, B to F′; quantification in S12G), and conditional removal of *PlexA2* in all SACs disrupts On, but not Off, ChAT^{+} dendritic

plexus organization (Fig. 4I and fig. S14, A and B). These results show that PlexA2 is cell-type–autonomously required for On, but not Off, SAC plexus organization.

To investigate the correlation between SAC morphological defects and function (22), we performed patch-clamp recordings from labeled On SACs in flat-mount retinas of *ChAT::cre;ROSA*$^{LSL\text{-}Tdtomato}$ mice in wild-type or *Sema6A*$^{-/-}$ genetic backgrounds. Although *Sema6A*$^{-/-}$ On SACs exhibit reduced dendritic length, coverage area, complexity, and symmetric organization (Fig. 3), the average amplitude of the light-evoked excitatory postsynaptic current (EPSC) is not different from wild-type (Fig. 5, A and B), showing that *Sema6A*$^{-/-}$ On SACs retain normal light-evoked excitatory responses. However, *Sema6A*$^{-/-}$ On SACs showed excess and aberrant light-evoked inhibitory postsynaptic currents (IPSCs) (fig. S15, A to C) mediated by γ-aminobutyric acid (GABA) receptors (fig. S15D). The mechanism underlying this change is presently unclear, although increased GABA-mediated lateral inhibition among *Sema6A*$^{-/-}$ On SACs is one likely possibility.

SACs are essential for retina direction-selectivity (23). Their radial symmetric dendritic morphology is likely to be essential for generating direction-selective responses from direction-selective ganglion cells (3). To assess any perturbations in direction-selective output due to SAC morphological defects, we performed cell-patch recordings, using two-photon microscopy to target neurons for electrophysiological analysis, in *TRHR-GFP;Sema6A*$^{+/-}$ and *TRHR-GFP;Sema6A*$^{-/-}$ mouse lines. In these mice On-Off direction-selective ganglion cells with posterior motion detection preference are genetically labeled by green fluorescent protein (GFP) (24). *TRHR-GFP;Sema6A*$^{+/-}$ direction-selective ganglion cells presented with drifting-bar motion stimulation displayed normal posterior-preferred directional tuning for both On and Off responses (Fig. 5C) (24). *TRHR-GFP;Sema6A*$^{-/-}$ direction selective ganglion cells, in contrast, showed compromised On direction-selective tuning (Fig. 5D, red line), although Off direction-selective tuning is preserved (Fig. 5D, blue line). Pooled data show that On responses in *TRHR-GFP;Sema6A*$^{-/-}$ direction-selective ganglion cells have abnormal, broader, directional tuning, with the magnitudes of the On response vector sums being significantly lower than in the control group (Fig. 5E, 0.15 ± 0.09 for *TRHR-GFP;Sema6A*$^{-/-}$ cells and 0.43 ± 0.20 for *TRHR-GFP;Sema6A*$^{+/-}$ cells, mean ± SD; $P < 0.01$, Mann-Whitney test). In contrast, *TRHRGFP; Sema6A*$^{-/-}$ Off direction-selective responses were not significantly broader than those observed in the control group (magnitude values of Off response vector sums: 0.32 ± 0.15 for *TRHR-GFP;Sema6A*$^{-/-}$ cells and 0.40 ± 0.15 for *TRHR-GFP;Sema6A*$^{+/-}$ cells; $P = 0.18$, Mann-Whitney test). Dye-fills of individual TRHR-GFP^{+} direction-selective ganglion cells reveal that *TRHRGFP; Sema6A*$^{-/-}$ DSGC dendrites still cofasciculate with On SAC dendritic processes (Fig. 5F and fig. S16), and the dendritic field area of *TRHRGFP; Sema6A*$^{-/-}$ direction-selective ganglion cells in both Off and On SAC plexuses does not differ from *TRHR-GFP;Sema6A*$^{+/-}$ direction-selective ganglion cells (fig. S17). Taken together, these results show that On directional tuning of at least one On-Off direction-selective ganglion cell subtype is defective in *Sema6A*$^{-/-}$ mutants.

In this study, we demonstrate that Sema6A, a classical axon guidance cue, is a molecular determinant that distinguishes On from Off visual pathways. Sema6A, together with PlexA2, regulates SAC dendritic stratification, On SAC dendritic morphology, and functional assembly of retinal direction-selective circuitry. In the neonatal murine retina, repulsive Sema6A-PlexA2 signaling disentangles On and Off SAC dendritic processes, providing the anatomical organization critical for the emergence and separation of On and Off direction-selective circuitry (Fig. 6A). Despite our observation of SAC inner plexiform layer stratification defects in all *Sema6A*$^{-/-}$ and *PlexA2*$^{-/-}$ mutant retinas examined, there remain normally stratified SAC processes in these mutants such that most SAC dendrites are still confined to their normal ChAT^{+} sublaminae, suggesting that additional dendritic

stratification mechanisms function in parallel to Sema6A-PlexA2 signaling to ensure proper SAC dendrite stratification. Our in vitro observation that exogenous Sema6A protein repels SAC neurites expressing PlexA2 but not Sema6A (corresponding to Off SACs), but does not affect SAC neurites expressing both PlexA2 and Sema6A(corresponding to On SACs), suggests that Sema6A and PlexA2 use in trans repulsion to facilitate correct SAC stratification. The lack of a repulsive response to exogenous Sema6A by SACs that express both Sema6A and PlexA2 likely reflects the silencing of PlexA2 by ligand expressed in cis, as has been observed in murine sensory neurons that express both Sema6A and PlexA4 and do not respond to exogenous Sema6A in vitro (25). Our data suggest that On SAC dendritic processes in vivo are not repelled by exogenous Sema6A, so defects in their laminar stratification in the inner plexiform layer may occur as a secondary consequence of Off SAC stratification defects or as a result of distinct Sema6A-PlexA2 signaling interactions.

During later postnatal retinal development, select and continuous expression of Sema6A in On SACs signals through PlexA2 to elaborate dendritic morphology, including symmetric organization of dendritic processes (Fig. 6B); apparently, Off SACs use molecular mechanisms distinct from those used by On SACs to achieve symmetric dendritic arbors. Sema6A-PlexA2 repulsion likely serves to separate rapidly growing On SAC dendritic processes from one another within the same SAC; however, these repulsive interactions must not occur among neighboring SACs. Sema6A-PlexA2 repulsive signaling may be constrained to early postnatal SACs when overlap with adjacent SAC dendritic processes is minimal, or it may be restricted to emerging dendritic branch points during the course of dendritic arbor growth. Therefore, it is critical to determine the spatial and temporal dynamics of plexin receptor activation during SAC development. In addition, protocadherin signaling (13), and likely additional mechanisms, also mediate SAC dendritic process self-avoidance and allow for intercellular SAC dendritic process overlap. Horizontal cells in the mouse retina express both Sema6A and another of its receptors, PlexA4, and horizontal cell dendrites in *PlexA4*$^{-/-}$ mutants show self-avoidance defects (15). Taken together, our data show that semaphorin ligands and their cognate receptors expressed in the same neuron facilitate the elaboration of dendritic arbors during postnatal retinal development.

Disruption of Sema6A-PlexA2 signaling leads to morphological deficits in On SACs and ultimately results in severely compromised On directional tuning in a subclass of direction-selective ganglion cells. Our elucidation of molecular events critical for functional assembly of retinal direction-selective circuitry may have general implications for understanding the establishment of circuitry in which individual neurons participate in multiple, distinct pathways.

Supplementary Material

Refer to Web version on PubMed Central for supplementary material.

Acknowledgments

We thank D. Ginty for the *ROSA*$^{\text{LSL-Tdtomato}}$ mice, J. Nathans for *Six3-cre*, *ChAT::cre*, *ChAT::cre*^{ER}, and *ROSA*^{iAP} mice, and Y. Yoshida for the *Sema6B*$^{-/-}$ and *Sema6C*$^{-/-}$;*6D*$^{-/-}$ eyes. We also thank S. Hattar, M. Riccomagno, and Q. Wang for comments on the manuscript and all Kolodkin laboratory members for assistance and discussions throughout the course of this project. This work was supported by NS35165 (A.L.K.); EY06837 (K.-W.Y.); EY019498 and EY013528 (M.B.F.); and the Human Frontier Science Program Organization, the National Postdoctoral Award Program for Advancing Women in Science, and the Edmond and Lily Safra (ELSC) Fellowship for postdoctoral training in Brain Science (M.R.-E.). A.L.K. is an investigator of the Howard Hughes Medical Institute.

References and Notes

1. Demb JB. Cellular mechanisms for direction selectivity in the retina. Neuron. 2007; 55:179–186. pmid: 17640521. [PubMed: 17640521]
2. Wei W, Feller MB. Organization and development of direction-selective circuits in the retina. Trends Neurosci. 2011; 34:638–645. pmid: 21872944. [PubMed: 21872944]
3. Vaney DI, Sivyer B, Taylor WR. Direction selectivity in the retina: Symmetry and asymmetry in structure and function. Nat. Rev. Neurosci. 2012; 13:194–208. pmid: 22314444. [PubMed: 22314444]
4. Masland RH. The neuronal organization of the retina. Neuron. 2012; 76:266–280. pmid: 23083731. [PubMed: 23083731]
5. Chalupa LM, Günhan E. Development of On and Off retinal pathways and retinogeniculate projections. Prog. Retin. Eye Res. 2004; 23:31–51. pmid: 14766316. [PubMed: 14766316]
6. Stacy RC, Wong ROL. Developmental relationship between cholinergic amacrine cell processes and ganglion cell dendrites of the mouse retina. J. Comp. Neurol. 2003; 456:154–166. pmid: 12509872. [PubMed: 12509872]
7. Huberman AD, et al. Genetic identification of an On-Off direction-selective retinal ganglion cell subtype reveals a layer-specific subcortical map of posterior motion. Neuron. 2009; 62:327–334. pmid: 19447089. [PubMed: 19447089]
8. Kay JN, et al. Retinal ganglion cells with distinct directional preferences differ in molecular identity, structure, and central projections. J. Neurosci. 2011; 31:7753–7762. pmid: 21613488. [PubMed: 21613488]
9. Euler T, Detwiler PB, Denk W. Directionally selective calcium signals in dendrites of starburst amacrine cells. Nature. 2002; 418:845–852. pmid: 12192402. [PubMed: 12192402]
10. Briggman KL, Helmstaedter M, Denk W. Wiring specificity in the direction-selectivity circuit of the retina. Nature. 2011; 471:183–188. pmid: 21390125. [PubMed: 21390125]
11. Wei W, Hamby AM, Zhou K, Feller MB. Development of asymmetric inhibition underlying direction selectivity in the retina. Nature. 2011; 469:402–406. pmid: 21131947. [PubMed: 21131947]
12. Yonehara K, et al. Spatially asymmetric reorganization of inhibition establishes a motion-sensitive circuit. Nature. 2011; 469:407–410. pmid: 21170022. [PubMed: 21170022]
13. Lefebvre JL, Kostadinov D, Chen WV, Maniatis T, Sanes JR. Protocadherins mediate dendritic self-avoidance in the mammalian nervous system. Nature. 2012; 488:517–521. pmid: 22842903. [PubMed: 22842903]
14. Matsuoka RL, et al. Class 5 transmembrane semaphorins control selective mammalian retinal lamination and function. Neuron. 2011; 71:460–473. pmid: 21835343. [PubMed: 21835343]
15. Matsuoka RL, et al. Guidance-cue control of horizontal cell morphology, lamination, and synapse formation in the mammalian outer retina. J. Neurosci. 2012; 32:6859–6868. pmid: 22593055. [PubMed: 22593055]
16. Suto F, et al. Interactions between plexin-A2, plexin-A4, and semaphorin 6A control lamina-restricted projection of hippocampal mossy fibers. Neuron. 2007; 53:535–547. pmid: 17296555. [PubMed: 17296555]
17. Renaud J, et al. Plexin-A2 and its ligand, Sema6A, control nucleus-centrosome coupling in migrating granule cells. Nat. Neurosci. 2008; 11:440–449. pmid: 18327254. [PubMed: 18327254]
18. Matsuoka RL, Sun LO, Katayama K, Yoshida Y, Kolodkin AL. Sema6B, Sema6C, and Sema6D expression and function during mammalian retinal development. PLoS ONE. 2013; 8:e63207. pmid: 23646199. [PubMed: 23646199]
19. Ford KJ, Feller MB. Assembly and disassembly of a retinal cholinergic network. Vis. Neurosci. 2012; 29:61–71. pmid: 21787461. [PubMed: 21787461]
20. Wong RO, Collin SP. Dendritic maturation of displaced putative cholinergic amacrine cells in the rabbit retina. J. Comp. Neurol. 1989; 287:164–178. pmid: 2477402. [PubMed: 2477402]
21. Lefebvre JL, Zhang Y, Meister M, Wang X, Sanes JR. Gamma-Protocadherins regulate neuronal survival but are dispensable for circuit formation in retina. Development. 2008; 135:4141–4151. pmid: 19029044. [PubMed: 19029044]

22. Peters BN, Masland RH. Responses to light of starburst amacrine cells. J. Neurophysiol. 1996; 75:469–480. pmid: 8822571. [PubMed: 8822571]

23. Yoshida K, et al. A key role of starburst amacrine cells in originating retinal directional selectivity and optokinetic eye movement. Neuron. 2001; 30:771–780. pmid: 11430810. [PubMed: 11430810]

24. Rivlin-Etzion M, et al. Transgenic mice reveal unexpected diversity of on-off direction-selective retinal ganglion cell subtypes and brain structures involved in motion processing. J. Neurosci. 2011; 31:8760–8769. pmid: 21677160. [PubMed: 21677160]

25. Haklai-Topper L, Mlechkovich G, Savariego D, Gokhman I, Yaron A. Cis interaction between Semaphorin6A and Plexin-A4 modulates the repulsive response to Sema6A. EMBO J. 2010; 29:2635–2645. pmid: 20606624. [PubMed: 20606624]

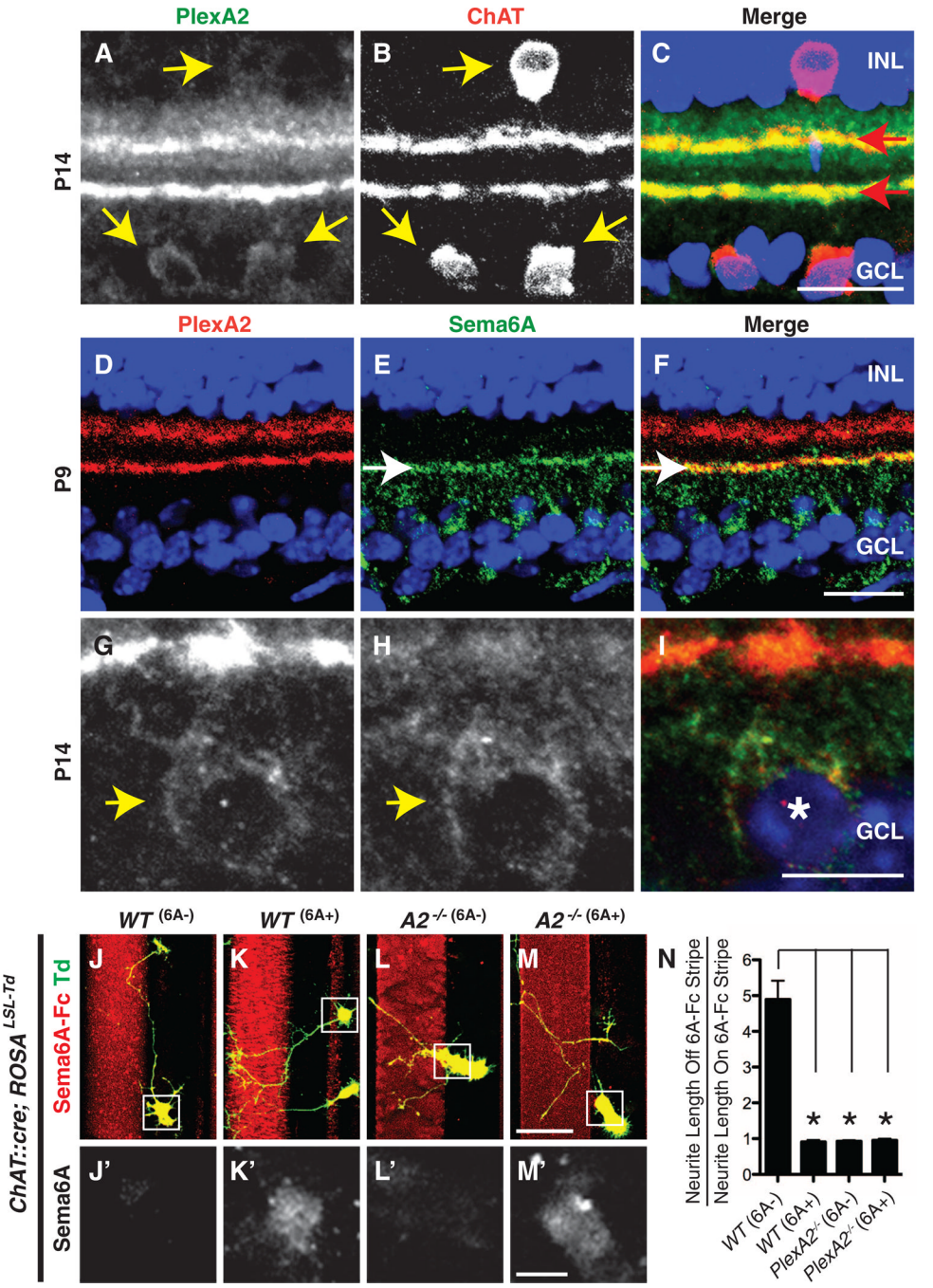

Fig. 1. Sema6Ais expressed in On, but not Off, SACs in vivo, and SACs lacking Sema6A avoid exogenous Sema6A in vitro

(**A** to **C**) Mouse P14 retina sections immunostained with antibodies directed against PlexA2 (green) and ChAT (red) reveal colocalization of PlexA2 and ChAT immunoreactivity in cell bodies (yellow arrows) and in dendritic processes (red arrows). (**D** to **I**) Postnatal retina sections immunostained with antibodies to PlexA2 (red) and antibodies to Sema6A (green) show that PlexA2 and Sema6A exhibit mostly complementary protein distributions in the inner plexiformlayer [white arrows in (E) and (F)] but that they are coexpressed in On SACs [yellow arrow heads in (G) and (H), white asterisk in (I)]. (**J** to **N**) Genetically labeled, dissociated SACs from wild-type (WT) retinas are divided into two populations in vitro:

Sema6A^{-} (J and J′) and Sema6A^{+} (K and K′). Neurites extending from WT Sema6A^{-} SACs avoid exogenous Sema6AFc stripes (J), whereas WT Sema6A^{+} SACs do not (K). *PlexA2*$^{-/-}$ SACs, both Sema6A^{+} and Sema6A^{-}, extend freely over Sema6A-Fc^{+} stripes [(L) and (M)]. The ratio of SAC neurite length off of Sema6AFc stripes to neurite length on Sema6A-Fc stripes is shown in (N) ($n \geq 15$ SACs per genotype). Error bars, mean ± SEM. *$P < 0.01$. Scale bars, 20 μm in (C) for (A) to (C), 20 μm in (F) for (D) to (F), 10 μm in (I) for (G) to (I), 40 μm in (M) for (J) to (M), and 10 μm in (M′) for (J′) to (M′).

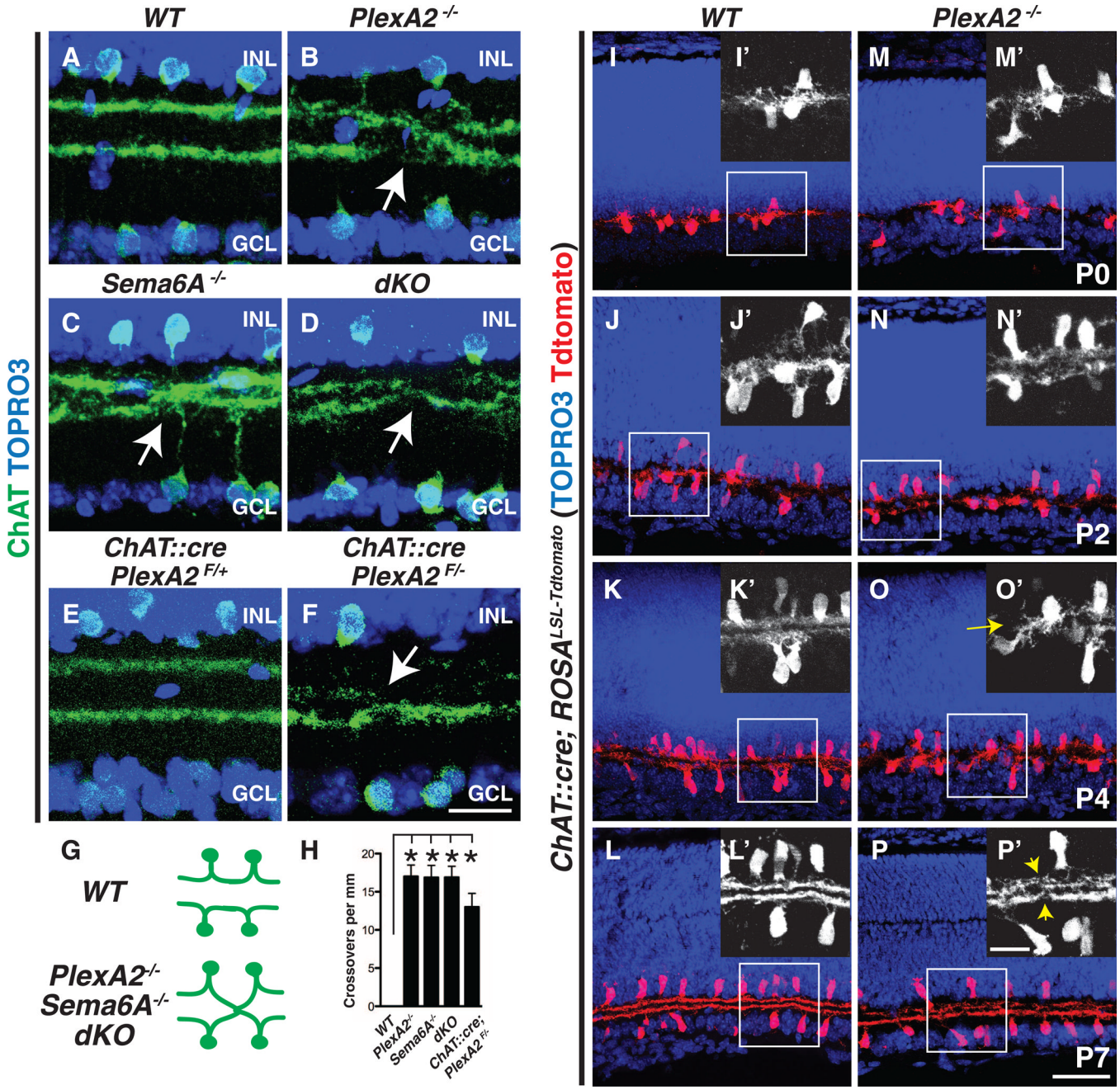

Fig. 2. Sema6A-PlexA2 signaling segregates On and Off SAC dendritic stratifications in vivo

(**A** to **D**) Wild-type (A), *PlexA2*$^{-/-}$ (B), *Sema6A*$^{-/-}$ (C), and *PlexA2*$^{-/-}$;*Sema6A*$^{-/-}$ (D) adult retina sections immunostained with antibodies to ChAT. On and Off SAC processes fail, with full penetrance, to completely segregate in *PlexA2*$^{-/-}$ (B), *Sema6A*$^{-/-}$ (C), and *PlexA2*$^{-/-}$;*Sema6A*$^{-/-}$ (D) retinas (stratification crossovers indicated by white arrows, $n \geq 4$ mice for each genotype). (**E** and **F**) Conditional removal of PlexA2 protein in SACs recapitulates *PlexA2*$^{-/-}$ stratification defects ($n = 3$ mice). (**G**) Schematics of SAC dendritic stratification in WT, *PlexA2*$^{-/-}$, *Sema6A*$^{-/-}$, and *PlexA2*$^{-/-}$; *Sema6A*$^{-/-}$ mutants. (**H**) Quantification of SAC stratification crossovers in (A) to (D) and in (F) ($n \geq 6$ retinas per genotype). Error bars, mean ± SD *$P < 0.001$. (**I** to **P′**) Characterization of SAC dendritic

stratification in WT [(I) to (L′)] and *PlexA2*$^{-/-}$ [(M) to (P′)] retinas using the SAC Tdtomato genetic reporter. In WT retinas, On and Off SAC dendrites are intermingled at P0 [(I) and (I′)]. They then segregate during early postnatal retinal development [(J) and (J′)] and become completely separate stratifications by P4 [(K) and (K′)]. SAC dendritic stratifications in *PlexA2*$^{-/-}$ mutants [(M), (M′), (N), and (N′)] are indistinguishable from WT [(I), (I′), (J), and (J′)] at P0 and at P2. However, the stratification phenotype is observed by P4 in *PlexA2*$^{-/-}$ retinas [(O) and (O′), yellow arrow)] and persists through P7 [(P) and (P′), yellow arrowheads]. n = 3 mice for each genotype at each different developmental stage. Scale bars, 20 μm in (F) for (A) to (F), 50 μm in (P) for (I) to (P), and 20 μm in (P′) for (I′) to (P′).

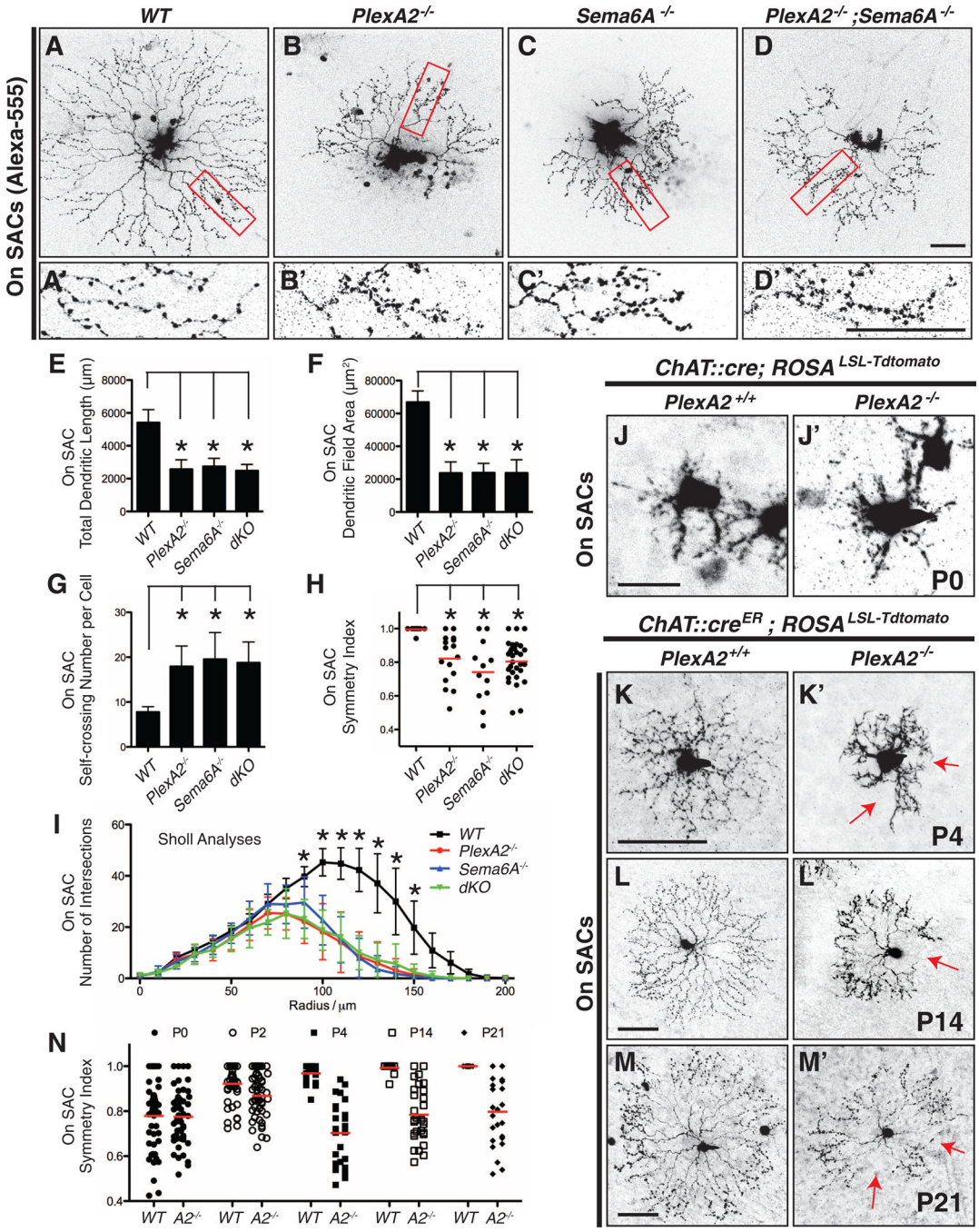

Fig. 3. Sema6A-PlexA2 signaling regulates dendritic arborization and symmetric organization in On SACs

(**A** to **D**) Single On SACs labeled with Alexa-555 in WT (A), *PlexA2*$^{-/-}$ (B), *Sema6A*$^{-/-}$ (C), and *PlexA2*$^{-/-}$;*Sema6A*$^{-/-}$ (D) adult retinas. (**A′** to **D′**) Single-plane confocal images of magnified fields in (A) to (D) (red rectangles) show that higher-order distal dendrites in *PlexA2*$^{-/-}$ (B′), *Sema6A*$^{-/-}$ (C′), and *PlexA2*$^{-/-}$;*Sema6A*$^{-/-}$ (D′) retinas exhibit self-avoidance defects in comparison with WT (A′). (**E** to **I**) Quantification of total dendritic length (E), dendritic field area (F), self-crossing number per cell (G), symmetry index (H), and dendritic complexity (I, measured by Sholl analyses) shows that overall dendritic morphology is disrupted in *PlexA2*$^{-/-}$, *Sema6A*$^{-/-}$, and *PlexA2*$^{-/-}$;*Sema6A*$^{-/-}$ retinas ($n \geq 12$

SACs per genotype). Error bars, mean ± SD. **P* < 0.01. (**J** to **M′**) Sparse genetic labeling of On SACs in WT retinas [(J) to (M)] shows that dendritic morphology of On SACs is not symmetric at P0 (J) but becomes symmetric during the course of early postnatal retinal development [(K) to (M)]. *PlexA2*$^{-/-}$ On SACs (J′) are indistinguishable from WT (J) at P0; however, they fail to establish dendritic process symmetry by P4 [red arrows in (K′)] and throughout retinal development [red arrows in (L′) and (M′)]. (**N**) Quantification of the symmetry index in WT and *PlexA2*$^{-/-}$ retinas through early postnatal retinal development. Red bars in (H) and (N) represent the mean value for each genotype. Scale bars, 50 μm in (D) for (A) to (D), 50 μm in (D′) for (A′) to (D′), 20 μm in (J) for (J) and (J′), 50 μm in (K) for (K) and (K′), 50 μm in (L) for (L) and (L′), and 50 μm in (M) for (M) and (M′).

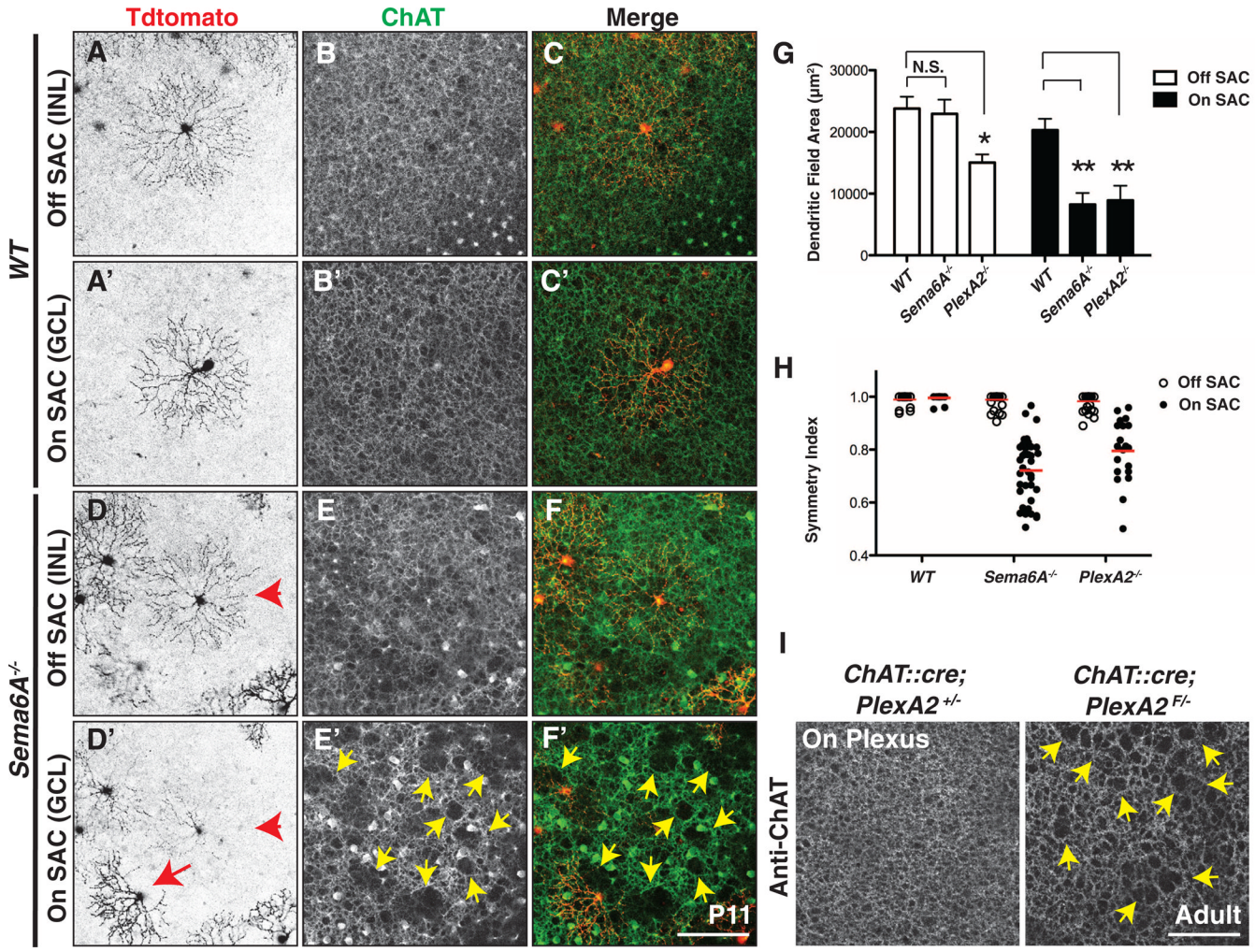

Fig. 4. Sema6A-PlexA2 signaling is dispensable for Off SAC dendritic arborization and ChAT^{+} plexus organization

(**A** to **F′**) Sparse genetic labeling of On [(A′) and (D′)] and Off [(A) and (D)] SACs coupled with anti-ChAT immunostaining of On [(B′) and (E′)] and Off [(B) and (E)] SAC dendritic plexuses in the same WT [(A) to (C′)] and *Sema6A*$^{-/-}$ [(D) to (F′)] retinas. (D) to (F) and (D′) to (F′) are different focal planes from the same field. On and Off SACs in WT retinas exhibit stereotypic symmetrical morphology [(A) and (A′)]. In contrast, overall dendritic organization of *Sema6A*$^{-/-}$ On SACs [(D′), red arrow], but not Off SACs [(D) and (D′), red arrowhead], is disrupted. Similarly, SAC plexus organization revealed by anti-ChAT immunostaining shows that only the *Sema6A*$^{-/-}$ On SAC plexus is compromised, as indicated by large gaps and holes [yellow arrowheads in (E′) and (F′)]. (**G** and **H**) Quantification of dendritic field area (G) and symmetry index (H) of WT, *Sema6A*$^{-/-}$, and *PlexA2*$^{-/-}$ On and Off SACs at P11. Red bars in (H) represent mean value for each genotype. Error bars, mean ± SD. **P* < 0.01; ***P* < 0.001. (**I**) Dendritic plexus organization of On SACs in control (left) and *ChAT::cre;PlexA2*$^{F/-}$ (right) retinas. Conditional removal of PlexA2 protein in all SACs disrupts On, but not Off (see fig. S14, A and B), SAC plexus (yellow arrowheads in right panel). Scale bars, 100 μm in (F′) for (A) to (F′), 100 μm in (I) for left and right panels.

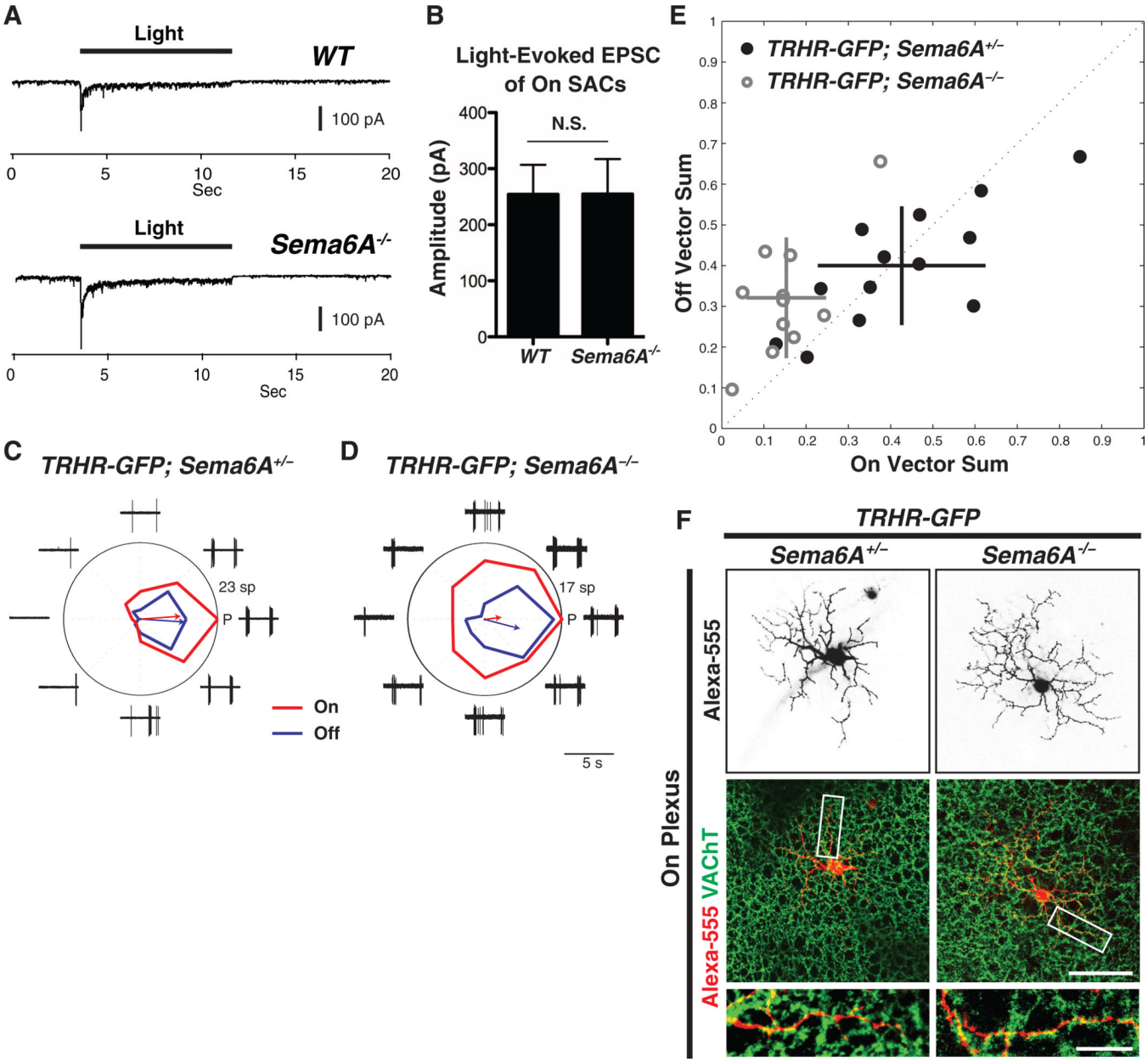

Fig. 5. On direction-selective tuning of bistratified TRHR-GFP^{+} direction-selective ganglion cells is compromised in *Sema6A*$^{-/-}$ mutants

(**A**) Representative light-evoked EPSC traces of WT (top) and *Sema6A*$^{-/-}$ (bottom) On SACs (voltage-clamped at −70 mV for both). Recordings from WT (n = 7) and *Sema6A*$^{-/-}$ (n = 8) On SACs show similar excitatory light responses. (**B**) The amplitude of light-evoked EPSCs is the same in WT and *Sema6A*$^{-/-}$ On SACs. Error bars, mean ± SEM. (**C** and **D**) Responses by TRHR-GFP^{+} On-Off direction-selective ganglion cells to drifting bars from individual *TRHR-GFP;Sema6A*$^{+/-}$ RGCs (C) and *TRHR-GFP; Sema6A*$^{-/-}$ RGCs (D). The red tuning curve shows the mean On response (spike count during On response phase), and the blue tuning shows the mean Off response (spike count during Off response phase); red and blue arrows indicate vector sums of the On and Off responses, respectively. Traces show the response data for one repetition of bar stimuli (5 s for each trial). P, posterior direction in visual coordinates; sp, total number of spikes. (**E**) On vector sum values versus

Off vector sum values for *TRHR-GFP;Sema6A*$^{+/-}$ cells (black filled circles) and *TRHR-GFP;Sema6A*$^{-/-}$ cells (gray rings). Horizontal and vertical lines represent SD values. (**F**) Alexa-555 dye-fills of individual TRHRGFP^{+} On-Off direction-selective ganglion cells and immunostaining with antibody to VAChT in P30 *Sema6A*$^{+/-}$ (left column) and *Sema6A*$^{-/-}$ mutants (right column) reveal that *TRHR-GFP;Sema6A*$^{-/-}$ On-Off direction-selective ganglion cells still cofasciculate with On SAC dendritic processes and display normal dendritic arbor morphology in the On plexus (also see fig. S16). Scale bars, 100 μm in the middle right panel of (F) for top and middle panels, 25 μm in the bottom right panel of (F) for the bottom two panels.

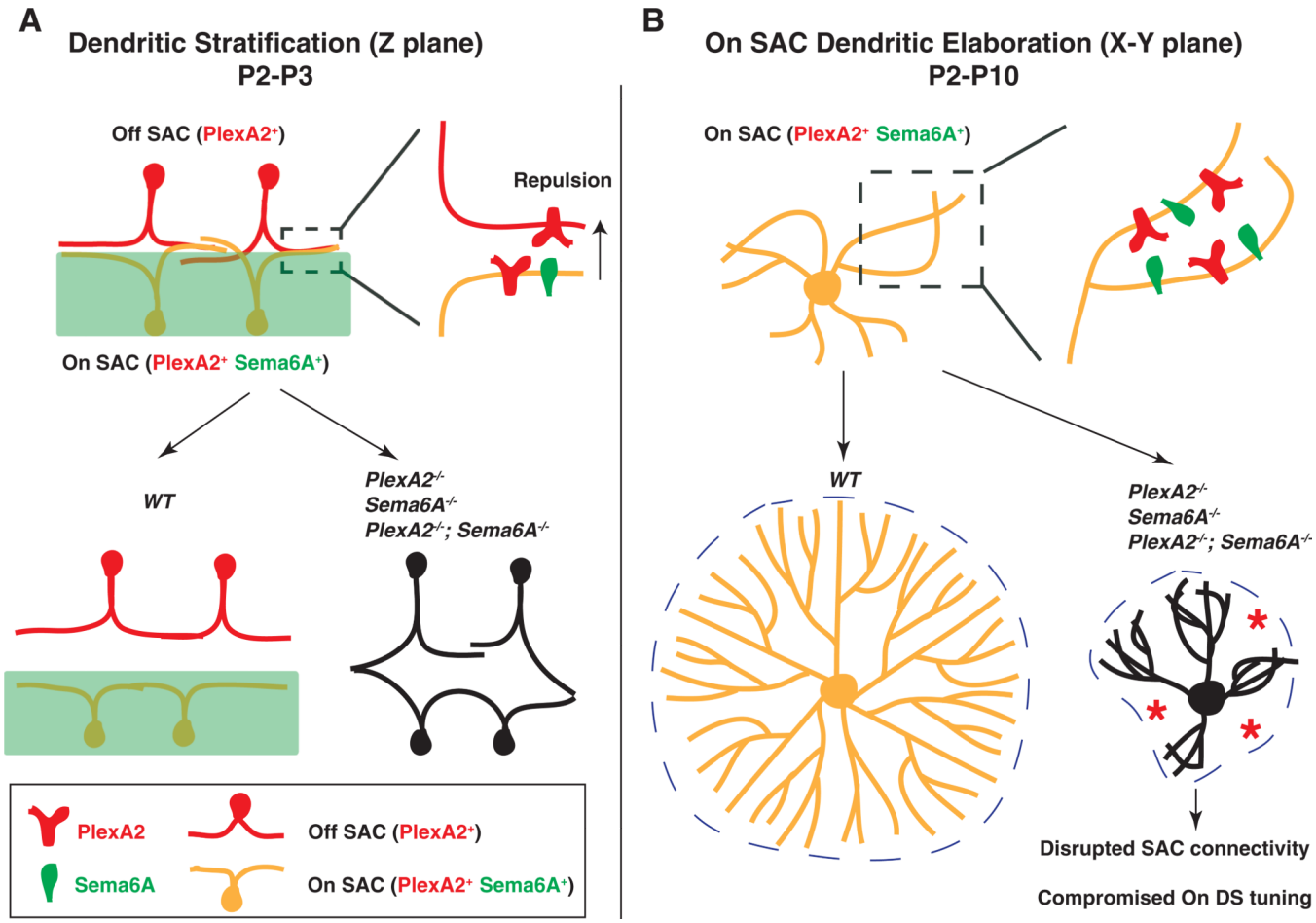

Fig. 6. Sema6A-PlexA2 signaling in the development of SACs and the functional assembly of direction-selective retinal circuits

Sema6A-PlexA2 signaling participates in two aspects of SAC development in the early postnatal mammalian retina. (**A**) In the *z* plane, PlexA2 is expressed in both On and Off SACs, whereas Sema6A is expressed only in the lower half of the inner plexiform layer and in On, but not Off, SACs. Repulsive Sema6A-PlexA2 signaling in trans segregates initially entangled On and Off SAC processes between P2 and P3. (**B**) In the *x-y* plane, continuous expression of both Sema6A and PlexA2 in On SACs functions to separate rapidly extending dendritic processes throughout early retinal development (P2 to P10). In WT retinas, On SACs are not symmetrically organized at P0. In the presence of intact Sema6A and PlexA2 signaling, On SAC dendrites avoid each other during this early phase of SAC dendritic development, leading to elaboration of symmetric SAC dendritic fields by the end of postnatal retinal development. In the absence of Sema6A, PlexA2, or both, many On SAC dendrites fail to fully separate from one another. This affects dendritic process dynamics and eventually causes dendritic field area and symmetry defects in *Sema6A*$^{-/-}$, *PlexA2*$^{-/-}$, and *Sema6A*$^{-/-}$;*PlexA2*$^{-/-}$ mutants. The disruption of On SAC dendritic plexuses affects GABA-mediated connectivity among On SACs and compromises directional tuning of On direction-selective responses.